

## New Directions in the Preparation and Redox Chemistry of Fluoride-Templated Tetranuclear Vanadium Phosphonate Cage Compounds, $M^{n+}[(V_2O_3)_2(RPO_3)_4CF]_n$

Jabor K. Jabor,<sup>\*,†</sup> Reinhard Stösser, Michael Feist, Petra Neubauer, and Manfred Meisel

Institut für Chemie, Humboldt-Universität zu Berlin, Brook-Taylor-Strasse 2, D-12489 Berlin, Germany

Received April 28, 2008

A new and simple preparation method for fluoride-templated tetranuclear vanadium phosphonate cage compounds,  $M^{n+}[(V_2O_3)_2(RPO_3)_4CF]_n$  is outlined. The crystalline products were characterized by X-ray diffraction, elemental analysis, and thermogravimetric analysis. Using the acceptable solubility of the products, multinuclear NMR could be performed on the corresponding solutions. Some insight into the process of formation of the cage compounds in solution could be reached by monitoring the corresponding reaction mixture by multinuclear NMR. The template function of the  $F^-$  ion could be demonstrated together with the fact that the non-transition-metal ions ( $M^{n+}$ ) used here (phosphonium ions) have no direct effect on the formation of the cage. In contrast, the redox behavior of these compounds in the solid state distinctly depends on the cations. This could be easily investigated by electron paramagnetic resonance because the mixed-valence species ( $3V^V/V^{IV}$ ) can be produced chemically or thermally induced in solution as well as in the solid state. In the latter case, the reaction of the cage with  $H_2$  activated on the platinum powder can be regarded as a *key experiment* for understanding the redox process of the title compounds in the solid state. The role of specific interactions in solution at the tumbling rate and the localization of spin density in the cage could be demonstrated by the reduction performed with 1-methylimidazole and quinoline. While the substituents  $R = Me$  and  $Ph$  have only a small influence on the cage formation in solution, they have a significant influence on the redox reaction and structural relaxation in the solid state.

### Introduction

There is a general problem in the field of solid-state chemistry as well as of heterogeneous catalysis if transition metals are involved: it is often difficult to give a clear answer concerning the structure of the active centers especially in such cases when they were produced by complex procedures such as calcination and formation. Soluble molecular metal oxides such as polyoxometalates<sup>1</sup> have received considerable attention because they can be considered as models for homogeneous and heterogeneous catalysis, while vanadium organophosphonate clusters have gained little attention because they are almost dense, nonsoluble, and nonporous

materials.<sup>2</sup> Therefore, in this paper we start from a molecular approach dealing with a new strategy of the synthesis of vanadium cage compounds. After a careful characterization of these species in solution, we transfer the gained electronic and structural knowledge to the solid state. In the first unique redox experiment, we will show that the structure of the active cage unit will be preserved. This means that the redox process can be performed reversibly with species of known structure even in the solid state.

Vanadium organophosphonates represent a large subclass of metal organophosphonates. On the basis of phosphonic acid derivatives, on the one hand, and vanadium oxygen species of different geometries and oxidation states, on the other hand, they combine the structural wealth of organic chemistry and the interesting redox properties of vanadium.<sup>3</sup>

\* To whom correspondence should be addressed. E-mail: jabor.jabor@catalysis.de.

† Current address: Leibniz-Institut für Katalyse eV an der Universität Rostock Aussenstelle Berlin, Richard-Willstätter-Strasse 12, D-12489 Berlin, Germany.

(1) *Polyoxometalates: From Platonic Solids to Anti-Retroviral Activity*; Pope, M. T., Müller, A., Eds.; Kluwer Academic Publishers: Dordrecht, The Netherlands, 1994.

(2) Mallouk, T.; Gavin, J. A. *Acc. Chem. Res.* **1998**, *31*, 209–217.

(3) Clearfield, A. Metal phosphonate chemistry. In *Progress in Inorganic Chemistry*; Karlin, K. D., Ed.; John Wiley & Sons: New York, 1998; Vol. 47, pp 371–510.

The ongoing development of vanadium organophosphonate chemistry stems not only from their structural diversity and interesting redox properties but also from potential applications in different areas such as catalysis<sup>4</sup> and intercalation.<sup>5</sup> One approach to prepare vanadium organophosphonate cage compounds is to use a chemical template, which provides the instructions for structural control and formation of the cage. A large number of templated compounds have been prepared in the presence of cationic, neutral, and anionic structure-directing groups.<sup>6</sup> In contrast to the cationic template, the anionic one has been developed more slowly. This is partially attributed to the intrinsic properties of anions such as larger radii, high polarizability, pH sensitivity, and their relatively high free solvation energies.<sup>7</sup> However, it has been demonstrated that the halide anions have a structure-directing role toward the organization of a wide range of vanadium organophosphonate cage compounds, e.g., F<sup>-</sup>,<sup>8–11</sup> Cl<sup>-</sup>,<sup>12–14</sup> and Br<sup>-</sup>.<sup>15</sup> The properties of halide anions such as their monatomic nature with spherical shape and variable size make them suitable ions to study their role in the formation of vanadium organophosphonate cage structures. Concerning the role of fluoride ions, Chen and Zubieta<sup>8</sup> and later Thorn et al.,<sup>9</sup> on the basis of the results of their synthesis, demonstrated that the fluoride ion has a template role toward the formation of the tetranuclear vanadium cage [(V<sub>2</sub>O<sub>3</sub>)<sub>2</sub>(RPO<sub>3</sub>)<sub>4</sub>CF]<sup>-</sup>, which is only formed in the presence of this anion. However, Carrano et al.<sup>16</sup> concluded that a template ion is not necessary for the formation of a tetranuclear vanadium cage. Accordingly, it seems important to know the chemistry associated with the reactions of vanadium(V) compounds, phosphonic acids, and the fluoride ion and its role in the construction of the [(V<sub>2</sub>O<sub>3</sub>)<sub>2</sub>(RPO<sub>3</sub>)<sub>4</sub>CF]<sup>-</sup> cages.

Generally, the progress in understanding the role of template anions is limited because of the fact that the solubility problem of the products prevents NMR studies in solution. Furthermore, most of the vanadium atoms in the cluster compounds are in either V<sup>IV</sup> or mixed (usually V<sup>IV</sup>/V<sup>V</sup>) oxidation states. Because V<sup>IV</sup> is paramagnetic, little or no structural information can be obtained from NMR spectroscopy. Further problems that prevent systematic

studies are the lack of suitable starting materials and the poor crystallinity of the final products. However, the cage compounds [(V<sub>2</sub>O<sub>3</sub>)<sub>2</sub>(RPO<sub>3</sub>)<sub>4</sub>CF]<sup>-</sup> offer fascinating properties to study the effect of *both* the fluoride ion for the formation of the cage structure and the organic moieties (either of phosphonate groups or of countercations) on the reactivity of the cage. This is partially due to the solubility of the cage structure in some organic solvents. As mentioned above, there are two methods known from the literature to prepare fluoride-templated vanadium cage compounds. Chen and Zubieta<sup>8</sup> have described the preparation of [NBu<sup>n</sup>]<sub>4</sub>[V<sub>4</sub>O<sub>6</sub>(PhPO<sub>3</sub>)<sub>4</sub>CF]·CH<sub>3</sub>CN from the reaction of [NBu<sup>n</sup>]<sub>4</sub>[V<sub>5</sub>O<sub>7</sub>(PhPO<sub>3</sub>)<sub>4</sub>]·2OCH<sub>3</sub> with an excess of HBF<sub>4</sub>·Et<sub>2</sub>O in CH<sub>3</sub>CN at room temperature, while Thorn et al.<sup>9</sup> prepared the compounds [Et<sub>4</sub>P][(V<sub>2</sub>O<sub>3</sub>)<sub>2</sub>(PhPO<sub>3</sub>)<sub>4</sub>CF], [Et<sub>4</sub>P][(V<sub>2</sub>O<sub>3</sub>)<sub>2</sub>(MePO<sub>3</sub>)<sub>4</sub>CF], and [Et<sub>4</sub>P][(V<sub>2</sub>O<sub>3</sub>)<sub>2</sub>(<sup>n</sup>BuOPO<sub>3</sub>)<sub>4</sub>CF] from the reaction of VO(O<sup>i</sup>Pr)<sub>3</sub> with PhPO<sub>3</sub>H<sub>2</sub>, MePO<sub>3</sub>H<sub>2</sub>, and <sup>n</sup>BuPO<sub>3</sub>H<sub>2</sub>, respectively, in methanol in the presence of [Et<sub>4</sub>P][AlF<sub>4</sub>] and water. In both cases, the starting vanadium compound and/or the source of the fluoride anion were of complex nature. From this point, it was of interest to have a simple method for preparing such kinds of materials in order to study the effect of the fluoride ion, the organic substitutes of the phosphonates, and the size, charge, and organic groups of the charge-compensating cations on the formation of the cage structure [(V<sub>2</sub>O<sub>3</sub>)<sub>2</sub>(RPO<sub>3</sub>)<sub>4</sub>CF]<sup>-</sup>.

It is therefore the aim of the present work (i) to outline a new strategy of synthesis, (ii) to give insight into the process of formation of the cage structure in solution assisted by the F<sup>-</sup> ion as a template controlled by NMR, (iii) to demonstrate the influence of the charge-compensating cations, and (iv) to show the unique possibilities of the redox behavior of the vanadium cage species by electron paramagnetic resonance (EPR) in solution and especially in the solid state at room temperature as well as in parallel with thermoanalytical studies.

## Experimental Section

**Synthesis.** A solution of 4 mmol of dioxodichlorovanadate M<sup>n+</sup>[VO<sub>2</sub>Cl<sub>2</sub>]<sub>n</sub>,<sup>17</sup> where M = Ph<sub>4</sub>P<sup>+</sup>, Ph<sub>3</sub>P(CH<sub>2</sub>)<sub>3</sub>Cl<sup>+</sup>, Ph<sub>3</sub>P(CH<sub>2</sub>)<sub>4</sub>Cl<sup>+</sup>, Ph<sub>3</sub>PCH<sub>2</sub>OCH<sub>3</sub><sup>+</sup>, (Et<sub>2</sub>N)<sub>3</sub>PCH<sub>2</sub>Ph<sup>+</sup>, Ph<sub>3</sub>PEt<sup>+</sup>, <sup>n</sup>Bu<sub>4</sub>P<sup>+</sup>, Ph<sub>3</sub>P(CH<sub>2</sub>)<sub>2</sub>PPh<sub>3</sub><sup>2+</sup>, or Ph<sub>3</sub>P(CH<sub>2</sub>)<sub>4</sub>PPh<sub>3</sub><sup>2+</sup>, in CH<sub>3</sub>CN (20 mL) was added to the hot suspension of 5 mmol of KF and 4.4 mmol of phosphonic acid in CH<sub>3</sub>CN (10 mL) with stirring for 10 min. A yellow-orange precipitate was formed directly or by slow evaporation of the solvent (in some cases, the addition of water causes precipitation of the product). The solid was collected, washed with a small amount of water and then with ether, and dried over silica gel in an exsiccator. The solid was recrystallized from acetonitrile to give the compounds listed in Table 2.

**Materials and Methods.** M<sup>n+</sup>[VO<sub>2</sub>Cl<sub>2</sub>]<sub>n</sub> compounds were prepared according to the slightly modified procedure appearing in the literature.<sup>18</sup> All other materials and solvents are commercially available.

<sup>19</sup>F and <sup>31</sup>P NMR spectra were measured on DPX 300 and <sup>51</sup>V NMR spectra on a Bruker AV 400 spectrometer. EPR spectra were

- (4) Vasylyev, M.; Neumann, R. *Chem. Mater.* **2006**, *18*, 2781–2783.
- (5) Johnson, W. J.; Jacobson, A. J.; Butler, W. M.; Rosenthal, S. E.; Brody, J. F.; Lewandowski, J. T. *J. Am. Chem. Soc.* **1989**, *111*, 381–383.
- (6) Finn, R. C.; Zubieta, J.; Haushalter, R. C. *Prog. Inorg. Chem.* **2003**, *51*, 421–601.
- (7) Vickers, M. S.; Beer, P. D. *Chem. Soc. Rev.* **2007**, *36*, 211–225.
- (8) Chen, Q.; Zubieta, J. *J. Chem. Soc., Chem. Commun.* **1994**, 2663–2666.
- (9) Thorn, D.; Harlow, R.; Herron, N. *Inorg. Chem.* **1995**, *34*, 2629–2638.
- (10) Thong, N. H.; Jabor, J. K.; Stösser, R.; Meisel, M.; Ziemer, B. *Eur. J. Inorg. Chem.* **2007**, *22*, 3582–3593.
- (11) Jabor, J. K.; Stösser, R.; Thong, N. H.; Meisel, M.; Ziemer, B. *Angew. Chem., Int. Ed.* **2007**, *46*, 6354–6356.
- (12) Salta, J.; Chen, Q.; Chang, Y.-D.; Zubieta, J. *Angew. Chem., Int. Ed. Engl.* **1994**, *33*, 757–760.
- (13) Chang, Y.-D.; Salta, J.; Zubieta, J. *Angew. Chem., Int. Ed. Engl.* **1994**, *33*, 325–327.
- (14) Chen, Q.; Zubieta, J. *J. Chem. Soc., Chem. Commun.* **1994**, 1635–1636.
- (15) Meisel, M. To be published.
- (16) Otieno, T. L.; Mokry, M.; Bond, M. R.; Carrano, C. J.; Dean, N. S. *Inorg. Chem.* **1996**, *35*, 850–856.

- (17) Jabor, J. K.; Meisel, M. To be published.
- (18) Ahlborn, E.; Diemann, E.; Müller, A. *J. Chem. Soc., Chem. Commun.* **1972**, *37*, 8–379.

**Table 1.**  $^{19}\text{F}$ ,  $^{31}\text{P}$ , and  $^{51}\text{V}$  NMR Parameters of  $\text{M}[(\text{V}_2\text{O}_3)_2(\text{RPO}_3)_4\text{CF}]$  DMSO- $d_6$  Solutions

no.	compound	yield, %	free phosphonic acid, ppm	$^{31}\text{P}$		$^{19}\text{F}$		$^{51}\text{V}$
				$\delta$ , ppm	$J$ , Hz	$\delta$ , ppm	$J$ , Hz	$\delta$ , ppm
1	$\text{Ph}_4\text{P}[(\text{V}_2\text{O}_3)_2(\text{MePO}_3)_4\text{CF}] \cdot 2\text{CH}_3\text{CN}$	74.4	25.5	34.5	1 6.0	-179.9	17.3	-590.0
2	$\text{Ph}_4\text{P}[(\text{V}_2\text{O}_3)_2(\text{PrPO}_3)_4\text{CF}]$	62.8	32.8	37.4	14.6	-177.7	15.3	-578.4
3	${}^t\text{Bu}_4\text{P}[(\text{V}_2\text{O}_3)_2(\text{BuPO}_3)_4\text{CF}]$	57.9	35.0	37.5	14.1	-177.8	14.7	-573.4
4	$\text{Ph}_3\text{P}(\text{CH}_2)_4\text{PPh}_3[(\text{V}_2\text{O}_3)_2(\text{BuPO}_3)_4\text{CF}]_2$	59.8	35.0	38.3	13.9	-178.7	14.7	-573.6
5	$\text{Ph}_4\text{P}[(\text{V}_2\text{O}_3)_2(\text{PhPO}_3)_4\text{CF}] \cdot \text{CH}_3\text{CN}$	80.1	14.6	21.3	13.0	-175.5	15.0	-580.4
6	$\text{Ph}_3\text{PCH}_2\text{CH}_3[(\text{V}_2\text{O}_3)_2(\text{PhPO}_3)_4\text{CF}]$	78.1	14.6	21.3	13.8	-175.5	15.2	-582.4
7	$\text{Ph}_3\text{PCH}_2\text{OCH}_3[(\text{V}_2\text{O}_3)_2(\text{PhPO}_3)_4\text{CF}]$	68.8	14.6	21.3	13.3	-175.5	15.0	-582.5
8	$\text{Ph}_3\text{P}(\text{CH}_2)_3\text{Cl}[(\text{V}_2\text{O}_3)_2(\text{PhPO}_3)_4\text{CF}]$	64.7	14.6	21.3	13.0	-175.5	15.3	-581.5
9	$\text{Ph}_3\text{P}(\text{CH}_2)_4\text{Cl}[(\text{V}_2\text{O}_3)_2(\text{PhPO}_3)_4\text{CF}]$	60.1	14.6	21.3	13.3	-175.6	15.3	-582.6
10	$(\text{Et}_2\text{N})_3\text{PCH}_2\text{Ph}[(\text{V}_2\text{O}_3)_2(\text{PhPO}_3)_4\text{CF}]$	60.9	14.6	21.3	13.4	-175.5	15.2	-582.4
11	$\text{Ph}_3\text{P}(\text{CH}_2)_2\text{PPh}_3[(\text{V}_2\text{O}_3)_2(\text{PhPO}_3)_4\text{CF}]_2$	70.5	14.6	21.3	12.3	-175.5	15.2	-582.1

**Table 2.** P–F and V–F Bond Lengths (Å) of  $\text{Ph}_4\text{P}[(\text{V}_2\text{O}_3)_2(\text{RPO}_3)_4\text{CF}]$  (R = Ph, Me,  ${}^i\text{Pr}$ ) Cages That Were Obtained from XRD

bond	$[(\text{V}_2\text{O}_3)_2(\text{PhPO}_3)_4\text{CF}]^-$	$[(\text{V}_2\text{O}_3)_2(\text{MePO}_3)_4\text{CF}]^-$	$[(\text{V}_2\text{O}_3)_2(\text{}^i\text{PrPO}_3)_4\text{CF}]^-$
P1–F1	2.8385	2.8457	2.8403
P2–F1	2.8322	2.8532	2.8417
P3–F1	2.8433		2.8369
P4–F1	2.8373		2.8542
average	2.8378	2.8494	2.8432
V1–F1	2.4340	2.4320	2.3912
V2–F1	2.4397	2.4307	2.4253
V3–F1	2.4306		2.4630
V4–F1	2.4547		2.4333
average	2.4397	2.4313	2.4282

measured on a ERS 300 spectrometer (ZWG/Magnettech GmbH, Berlin-Adlershof, Germany). The thermal analyses for the compounds  $\{[(\text{CH}_3\text{CH}_2)_2\text{N}]_3\text{PCH}_2\text{Ph}[(\text{V}_2\text{O}_3)_2(\text{PhPO}_3)_4\text{F}]\}$ ,  $\text{Ph}_3\text{P}(\text{CH}_2)_2\text{-PPh}_3[(\text{V}_2\text{O}_3)_2(\text{PhPO}_3)_4\text{F}]_2$ ,  $\text{Ph}_4\text{P}[(\text{V}_2\text{O}_3)_2(\text{PhPO}_3)_4\text{F}] \cdot \text{CH}_3\text{CN}$ , and  $\text{Ph}_4\text{P}[(\text{V}_2\text{O}_3)_2(\text{CH}_3\text{PO}_3)_4\text{F}] \cdot 2\text{CH}_3\text{CN}$  were performed on a STA 409 C (Netzsch Gerätebau GmbH, Selb, Germany) under a  $\text{N}_2$  atmosphere with a heating rate of  $10^\circ\text{C min}^{-1}$ . A thermogravimetric analysis (TGA) sample-holder system (Pt/PtRh10 thermocouple) was used.

X-ray: Data collection was carried out on an IPDS diffractometer (Stoe & Cie) at 180 K using graphite-monochromated Mo K $\alpha$  radiation and a cryostream cooler (Oxford Cryosystems). The data set was collected in steps of  $\Delta\varphi = 1.1^\circ$  up to  $198^\circ$ . The structure was solved<sup>19</sup> and refined<sup>20</sup> with the *SHELX 97* program.

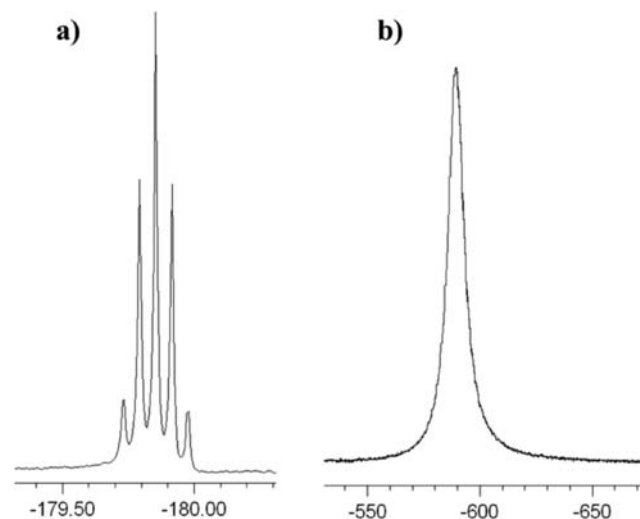
## Results and Discussion

**Synthesis.** A series of the cage compounds of the general formula  $\text{M}^{n+}[(\text{V}_2\text{O}_3)_2(\text{RPO}_3)_4\text{CF}]_n$  with  $\text{M} = \text{Ph}_4\text{P}^+$ ,  $\text{Ph}_3\text{P}(\text{CH}_2)_3\text{Cl}^+$ ,  $\text{Ph}_3\text{P}(\text{CH}_2)_4\text{Cl}^+$ ,  $\text{Ph}_3\text{PCH}_2\text{OCH}_3^+$ ,  $(\text{Et}_2\text{N})_3\text{PCH}_2\text{Ph}^+$ ,  $\text{Ph}_3\text{PEt}^+$ ,  ${}^t\text{Bu}_4^+$ ,  $\text{Ph}_3\text{P}(\text{CH}_2)_2\text{PPh}_3^{2+}$ , and  $\text{Ph}_3\text{P}(\text{CH}_2)_4\text{PPh}_3^{2+}$  and R = H, Me,  ${}^i\text{Bu}$ , and Ph were prepared by a new and very simple method (Table 1). The method involves the mixing of  $\text{M}[\text{VO}_2\text{Cl}_2]$  as a source of both vanadium and charge-compensating groups with phosphonic acid in the presence of a fluoride source (for simplicity, KF has been chosen; other salts also can be used such as tetraalkylammonium fluoride) in acetonitrile. The success of this reaction was confirmed by monitoring the multinuclear NMR ( $^{19}\text{F}$ ,  $^{31}\text{P}$ , and  $^{51}\text{V}$ ) spectra, the isolation and characterization of the solid complexes by means of elemental analysis, TGA, X-ray

diffraction (XRD), and multinuclear NMR ( $^{19}\text{F}$ ,  $^{31}\text{P}$ , and  $^{51}\text{V}$ ) analysis, which can be used for a certain characterization and confirmation of the existence of the cage structure in solution.

**NMR Spectroscopic Characterization.** Multinuclear NMR ( $^{19}\text{F}$ ,  $^{31}\text{P}$ , and  $^{51}\text{V}$ ) spectra were measured after dissolution of the solid complexes in DMSO- $d_6$ . The NMR data that are collected in Table 1 were used to confirm the existence of the cage structures  $[(\text{V}_2\text{O}_3)_2(\text{RPO}_3)_4\text{CF}]^-$  in solution. The  $^{51}\text{V}$  NMR spectra (Figure 1b) show only one signal in the range of  $-570$  to  $-590$  ppm, which indicates that all vanadium atoms of the cage have a similar magnetic environment in solution. However, there are small differences ( $\approx 20$  ppm) in the chemical shifts of  $^{51}\text{V}$  NMR nuclei of different cage structures. These differences are mainly due to the presence of different organic substituents of the phosphonate ligands  $[(\text{V}_2\text{O}_3)_2(\text{RPO}_3)_4\text{CF}]^-$  (R = Me,  ${}^i\text{Pr}$ ,  ${}^t\text{Bu}$ , or Ph), which result in small differences in the electronic environment around the vanadium atoms caused by the presence of a different bond nature between the phosphonate oxygen atoms and the vanadium ions (see below).

The  $^{31}\text{P}$  NMR signals of the phosphonate groups are shifted downfield relative to the corresponding free phosphonic acid and appear as a doublet with coupling constants of  ${}^1J = 12\text{--}15$  Hz (Figure 2). One possible cause for such splitting would be the coupling to the fluoride atom. The  $^{19}\text{F}$  NMR signal appears as a quintet in the range of  $-175$  to  $-180$

**Figure 1.** NMR spectra of  $\text{Ph}_4\text{P}[(\text{V}_2\text{O}_3)_2(\text{CH}_3\text{PO}_3)_4\text{CF}] \cdot 2\text{CH}_3\text{CN}$ : (a)  $^{19}\text{F}$  NMR; (b)  $^{51}\text{V}$  NMR in DMSO- $d_6$  (chemical shifts in ppm).

(19) Sheldrick, G. M. *Acta Crystallogr., Sect. A* **1990**, *46*, 467–473, cited for *SHELXS*.

(20) Sheldrick, G. M. *SHELXL-97, Program for Crystal Structure Refinement*; University of Göttingen: Göttingen, Germany, 1997.

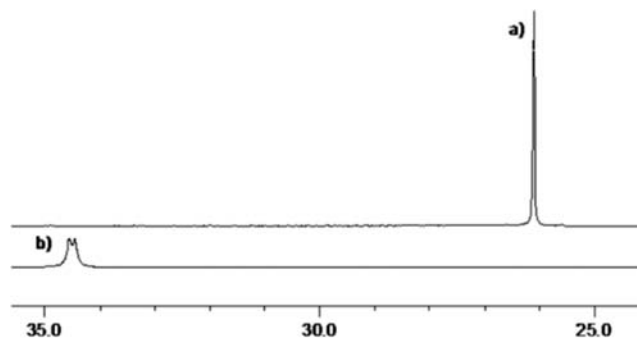


**Figure 2.**  $^{31}\text{P}$  NMR spectra of  $\text{MePO}_3\text{H}_2$  in  $\text{DMSO}-d_6$ : (a) free; (b) after formation of the cage complex  $\text{Ph}_4\text{P}[(\text{V}_2\text{O}_3)_2(\text{MePO}_3)_4\text{CF}] \cdot 2\text{CH}_3\text{CN}$  (chemical shifts in ppm).

ppm (Figure 1a) with a coupling constant of  $^1J \approx 15$  Hz, confirming the coupling effect. However, the crystallographic data (Table 2) of the cages  $\text{Ph}_4\text{P}[(\text{V}_2\text{O}_3)_2(\text{RPO}_3)_4\text{CF}]$  ( $\text{R} = \text{Me}, ^i\text{Pr}, \text{or Ph}$ ) show that the average distances between the encapsulated fluoride anion and the phosphonate phosphorus atoms are longer than the average distances between the fluoride and vanadium atoms, which are also parts of the cage. This means that the  $^{19}\text{F}$  nucleus also should be coupled with the  $^{51}\text{V}$  nuclei of the cage. Experimentally, this could not be resolved because of the broadening of the  $^{51}\text{V}$  NMR signal, which is caused by the quadruple relaxation of vanadium nuclei.

The values of the observed coupling constants suggest that a weak interaction takes place between the corresponding phosphorus located at the poles of the cage and the encapsulated fluoride anion via a direct through-space route. Furthermore, the small differences in the chemical shifts of  $^{19}\text{F}$ ,  $^{31}\text{P}$ , and  $^{51}\text{V}$  NMR spectra of different cage structures suggest that the organic residue of the phosphonate groups has a measurable effect on this shift. The  $^{31}\text{P}$  NMR signal positions of the charge-compensating phosphonium ions are in the same positions of the starting compounds, which indicates that the phosphonium ions are well separated from their counterpart, the cage structure.

The downfield shifts of the phosphorus atoms of phosphonate groups are attributed to the decrease of the P–O  $\pi$ -bonding character when the oxygen atoms are bonded to vanadium atoms. This is also reflected in the chemical shifts of the  $^{51}\text{V}$  NMR signals in the series of  $[(\text{V}_2\text{O}_3)_2(\text{MePO}_3)_4\text{CF}]^-$ ,  $[(\text{V}_2\text{O}_3)_2(^i\text{PrPO}_3)_4\text{CF}]^-$ , and  $[(\text{V}_2\text{O}_3)_2(\text{BuPO}_3)_4\text{CF}]^-$ , which are shown in Table 1. The steric and electronic influences of the organic substituents at the phosphonate groups probably are responsible for the relatively small differences in the chemical shifts of the vanadium nuclei. The highest downfield shift should indicate the smallest P–O  $\pi$  character.

**Structures.** Vanadium organophosphonate molecular compounds are built from the connection between the phosphonate ligands ( $\text{RPO}_3\text{H}_2$ ) and the vanadium oxide species. However, because of the structural diversity of vanadium oxygen polyhedral species, there are several types of connections between them and the phosphonate ligand. A fluoride template provides one tool for the construction of small cage compounds, i.e.,  $[(\text{V}_2\text{O}_3)_2(\text{RPO}_3)_4\text{F}]^-$ . The cage

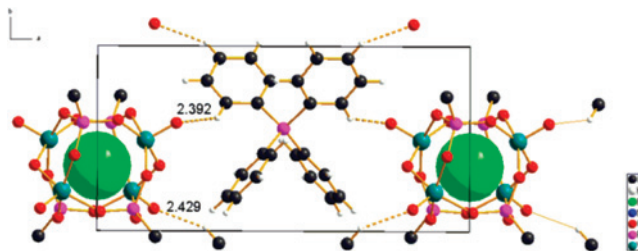


**Figure 3.** Crystal structure of the  $\text{Ph}_4\text{P}[(\text{V}_2\text{O}_3)_2(\text{MePO}_3)_4\text{CF}] \cdot 2\text{CH}_3\text{CN}$  complex showing the fluoride anions (with van der Waals radii) in the center of the cage and the hydrogen bonds.

structure can be regarded as a spherical molecule built around the fluoride anion with an internal surface made by the connections of vanadium and phosphorus atoms with oxygen atoms. Because of the steric effect, the organic rests that are pointing out of the cage surface play a crucial role in the determination of the redox activity of the cage.<sup>11</sup> Therefore, the structures of  $\text{Ph}_4\text{P}[(\text{V}_2\text{O}_3)_2(\text{MePO}_3)_4\text{CF}] \cdot 2\text{CH}_3\text{CN}$ ,  $\text{Ph}_4\text{P}[(\text{V}_2\text{O}_3)_2(^i\text{PrPO}_3)_4\text{CF}]$ , and  $\text{Ph}_4\text{P}[(\text{V}_2\text{O}_3)_2(\text{PhPO}_3)_4\text{CF}] \cdot \text{CH}_3\text{CN}$  were determined from single-crystal X-ray crystallographic analyses.

$\text{Ph}_4\text{P}[(\text{V}_2\text{O}_3)_2(\text{MePO}_3)_4\text{CF}] \cdot 2\text{CH}_3\text{CN}$  crystallizes in the monoclinic space group  $P12/c1$ . It is built up from a discrete cationic  $\text{Ph}_4\text{P}^+$  fragment and the anionic cage  $[(\text{V}_2\text{O}_3)_2(\text{CH}_3\text{PO}_3)_4\text{CF}]^-$  (Figure 3). The anionic and cationic fragments are held together by weak hydrogen bonds between the hydrogen atoms of the phenyl groups of the phosphonium ions and the oxygen atoms of the cage structure, as shown in Figure 3. The cage itself, which was described in the literature,<sup>9</sup> consists of four  $\text{CH}_3\text{PO}_3$  tetrahedra and four distorted  $\text{VO}_5$  square pyramids. Each of the two vanadium atoms share one oxygen atom to form the  $\text{V}_2\text{O}_3$  unit in which the axial oxygen atoms are in the trans position to each other. Each  $\text{CH}_3\text{PO}_3$  shares three oxygen atoms with three different VO groups, making a small cage cluster in which the fluoride anion is located almost in the center of the cage and directly in the opposite site of the  $\text{V}=\text{O}$  bonds.

Each  $\text{VO}_5$  unit has three kinds of oxygen atoms, namely, the terminal oxygen ( $d_{\text{V}-\text{O}} \approx 1.578\text{--}1.580$  Å), bridging oxygen VOV ( $d_{\text{V}-\text{O}} \approx 1.801\text{--}1.809$  Å), and VOP ( $d_{\text{V}-\text{O}} \approx 1.9162\text{--}1.939$  Å). The distances between the fluoride and vanadium ions ( $\approx 2.431$  Å) are a little larger than that of the usual  $\text{V}^{\text{V}}\text{--F}$  bond ( $\approx 1.8$  Å), but they are smaller than the sum of van der Waals radii of the fluoride and vanadium ions, which indicates that there is a weak electrostatic interaction between them. The P–O distances are in the range of  $1.526\text{--}1.543$  Å, which are expected for three coordinated phosphonate compounds.

The anionic cage structures of  $\text{Ph}_4\text{P}[(\text{V}_2\text{O}_3)_2(^i\text{PrPO}_3)_4\text{CF}]$  and  $\text{Ph}_4\text{P}[(\text{V}_2\text{O}_3)_2(\text{PhPO}_3)_4\text{CF}]$  are, in principle, similar to that of  $\text{Ph}_4\text{P}[(\text{V}_2\text{O}_3)_2(\text{MePO}_3)_4\text{CF}] \cdot 2\text{CH}_3\text{CN}$ . However, they belong to different crystal systems and/or space groups. For example,  $\text{Ph}_4\text{P}[(\text{V}_2\text{O}_3)_2(^i\text{PrPO}_3)_4\text{CF}]$  (Figure 4) crystallizes in the monoclinic space group  $P121/n1$ , while  $\text{Ph}_4\text{P}[(\text{V}_2\text{O}_3)_2(\text{PhPO}_3)_4\text{CF}]$  (Figure 5) crystallizes in the orthorhombic space group  $Pca21$ .

The average distances between the fluoride and vanadium ions, which are located at the poles of the cage struc-



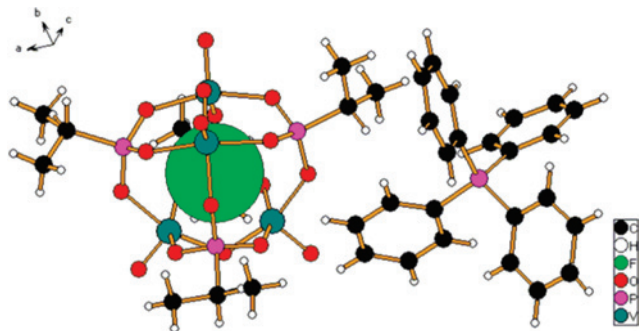


**Figure 4.** Crystal structure of the  $\text{Ph}_4\text{P}[(\text{V}_2\text{O}_3)_2(\text{iPrPO}_3)_4\text{F}]$  complex showing the fluoride anion with a van der Waals radius.

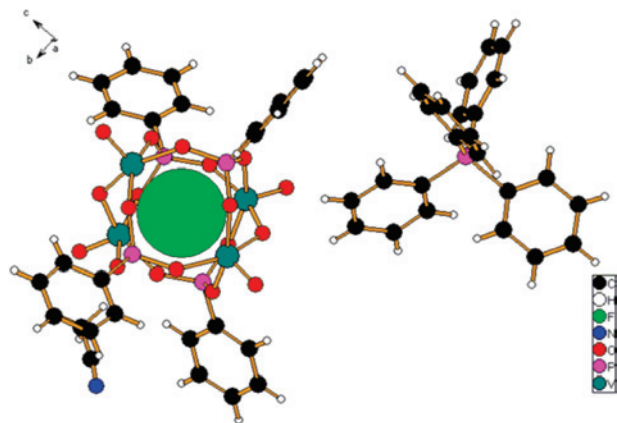


**Figure 5.** Crystal structure of the  $\text{Ph}_4\text{P}[(\text{V}_2\text{O}_3)_2(\text{PhPO}_3)_4\text{CF}] \cdot \text{CH}_3\text{CN}$  complex showing the fluoride anion with a van der Waals radius.

tures  $\text{Ph}_4\text{P}[(\text{V}_2\text{O}_3)_2(\text{MePO}_3)_4\text{CF}] \cdot 2\text{CH}_3\text{CN}$ ,  $\text{Ph}_4\text{P}[(\text{V}_2\text{O}_3)_2(\text{iPrPO}_3)_4\text{CF}]$ , and  $\text{Ph}_4\text{P}[(\text{V}_2\text{O}_3)_2(\text{PhPO}_3)_4\text{CF}] \cdot \text{CH}_3\text{CN}$  are 2.439, 2.431, and 2.428 Å, respectively. The small differences in the V–F distances indicate that the cage structures have similar volumes. However, a careful examination of the bond distances (Table 2) between the fluoride anion and the vanadium atoms, as well as the phosphonate phosphorus atoms, suggests that the fluoride anion is not located exactly in the center of the cage and its position is slightly different from one cage to another. For example, the position of the fluoride anion is less symmetrically fixed in the middle of the cage structure in  $\text{Ph}_4\text{P}[(\text{V}_2\text{O}_3)_2(\text{PhPO}_3)_4\text{CF}] \cdot \text{CH}_3\text{CN}$  than in  $\text{Ph}_4\text{P}[(\text{V}_2\text{O}_3)_2(\text{MePO}_3)_4\text{CF}] \cdot 2\text{CH}_3\text{CN}$ . This distortion in the solid state is likely due to the packing effect. The vanadium ion positions are raised above their basal planes toward the terminal oxygen atom. An attempt to find a correlation between the bond length of V–F and the *trans*-vanadyl oxygen atoms failed. This may be due to the small differences in the bond length and the packing effect in the solid state. As shown in Table 2, the fluoride ion is not totally disposed in the center of the cavity of the cage structure.

**Active Role of the Fluoride Anion as a Template and the Possible Function of a Cation in the Formation of the Cage Structures.** To obtain information about the role of the fluoride anion as a templating agent and about the influence of the type of counteranion in the formation of the tetranuclear vanadium cage  $[(\text{V}_2\text{O}_3)_2(\text{MePO}_3)_4\text{CF}]^-$ , the reaction mixture of  $\text{M}[\text{VO}_2\text{Cl}_2]$ ,

$\text{MePO}_3\text{H}_2$ , and  $\text{KF}$  (in an excess) in  $\text{CD}_3\text{CN}$  was investigated by measuring the multinuclear NMR spectra  $^{19}\text{F}$ ,  $^{31}\text{P}$ , and  $^{51}\text{V}$  (Table 3). The  $^{51}\text{V}$  NMR spectra of the starting materials  $\text{M}[\text{VO}_2\text{Cl}_2]$  exhibit only one signal at  $-365$  ppm, which shifts to a high field ( $-594$  ppm) upon reaction with methylphosphonic acid and  $\text{KF}$ . The disappearance of the  $^{51}\text{V}$  NMR signal of the starting compound indicates that all vanadium atoms have been reacted to form a new species in which all vanadium atoms have a magnetically equivalent environment. The strong high-field chemical shift ( $\approx 225$  ppm) of the  $^{51}\text{V}$  NMR signal in solution should be attributed to a change in the coordination sphere of the vanadium ions from the distorted tetrahedral of the starting compound  $\text{M}[\text{VO}_2\text{Cl}_2]$  to pseudooctahedral  $\text{VO}_5\text{F}$ .<sup>21</sup> A comparison between the  $^{51}\text{V}$  NMR signals obtained from this reaction and those of  $\text{Ph}_4\text{P}[(\text{V}_2\text{O}_3)_2(\text{MePO}_3)_4\text{CF}]$  gives a hint about the formation of the cage structure. It is noteworthy that, in the absence of  $\text{F}^-$ , the mixture of  $\text{Ph}_4\text{P}[\text{VO}_2\text{Cl}_2]$  and  $\text{MePO}_3\text{H}_2$  gives no relevant changes in the positions of the NMR signals under the same reaction conditions. The  $^{31}\text{P}$  NMR spectrum of the reaction mixture exhibits a low-field-shifted signal in comparison with that of free phosphonic acid. This shift is attributed to the coordination of phosphonate oxygen atoms with vanadium ions, which should result in a weakening of the P=O bond. This assumption was supported by elongation of the P–O bond lengths, which were obtained from the single-crystal X-ray measurements. The  $^{19}\text{F}$  NMR spectrum of the same mixture exhibits two signals. One, with a high chemical shift of  $-180.7$  ppm, appears as a quintet, which was attributed to P–F coupling of the encapsulated fluoride anion with the four phosphorus atoms in the cage structure. The other signal appears as a singlet at  $-152$  ppm. This signal was assigned to  $\text{BF}_4^-$ ,<sup>22</sup> which was obviously formed from the NMR glass tube in the presence of fluoride anions or  $\text{HF}$ .

The  $^{31}\text{P}$ ,  $^{19}\text{F}$ , and  $^{51}\text{V}$  NMR results (Figure 6) clearly show that only one kind of vanadium species has formed, i.e., the cage compound. Concerning the role of the  $\text{F}^-$  ion, it could be stated that the interaction of  $\text{KF}$  with phosphonic acid results in the formation of  $\text{HF}$ , which will interact in situ with  $[\text{VO}_2\text{Cl}_2]^-$  to form different vanadium–fluoride intermediates either through an addition reaction and/or exchange with a chloride ion. Both the addition and the exchange reactions were confirmed by Hibbert in 1986<sup>23</sup> for vanadium–fluoride species. Keeping in mind that the fluoride ion is a strong ligand for vanadyl species<sup>24</sup> because of its small size with a high charge density that could be easily diminished by coordination with a vanadium ion, which has energetically available vacant orbitals. Obviously, under the above-mentioned reaction conditions, the reaction rate for the formation of the cage compound is fast enough that no hint for the formation of intermediates like oxofluorinated vanadium species is found. The  $^{19}\text{F}$  NMR spectrum of the

(21) Donnel, S. E. D.; Pope, M. T. *J. Chem. Soc., Dalton Trans.* **1976**, 21, 2290–2297.

(22) Fairhurst, S. A.; Hughes, D. L.; Leigh, G. J.; Sanders, J. R.; Weisner, J. *J. Chem. Soc., Dalton Trans.* **1994**, 259, 1–2598.

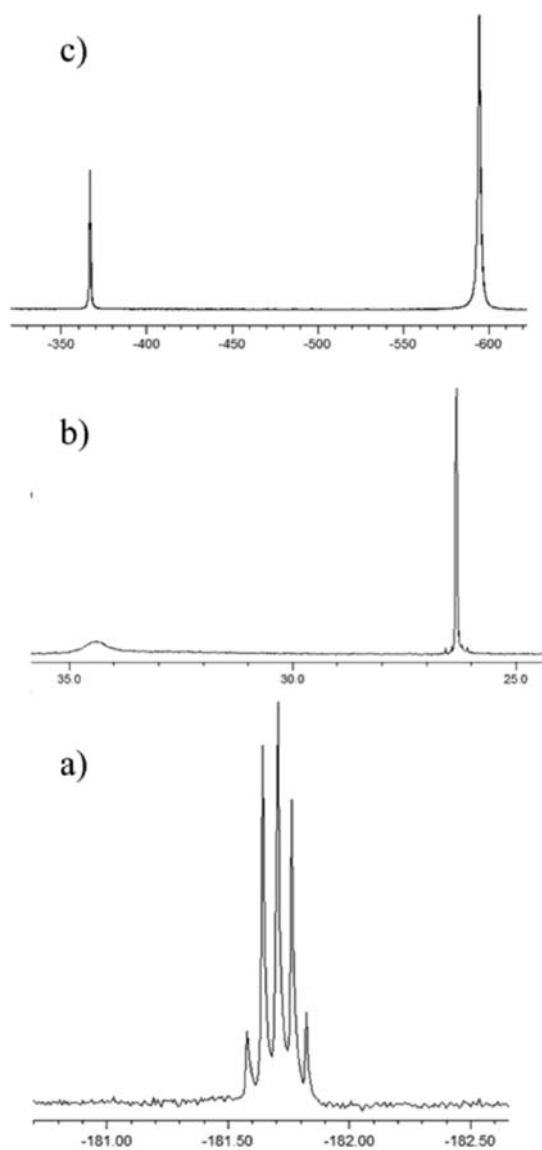
(23) Hibbert, R. C. *J. Chem. Soc., Dalton Trans.* **1986**, 751–753.

(24) Selbin, J. *Chem. Rev.* **1965**, 65, 153–175.

**Table 3.**  $^{19}\text{F}$ ,  $^{31}\text{P}$ , and  $^{51}\text{V}$  NMR Parameters of the Reaction Mixture of  $\text{M}[\text{VO}_2\text{Cl}_2]$  (0.1 mmol),  $\text{KF}$ , and  $\text{MePO}_3\text{H}_2$  (0.1 mmol) in  $\text{CD}_3\text{CN}$  at Room Temperature (Only of the Cage Structure, Chemical Shifts in ppm)

no.	$\text{M}[\text{VO}_2\text{Cl}_2]$	$^{31}\text{P}$ phosphonate		$^{19}\text{F}$		$^{51}\text{V}$
		$\delta$ , ppm		$\delta$ , ppm	$J$ , Hz	$\delta$ , ppm
1	$\text{Ph}_4\text{P}[\text{VO}_2\text{Cl}_2]$	34.7		-180.6 q	17.0	-594.4
2	$\text{Ph}_3\text{PCH}_2\text{OCH}_3[\text{VO}_2\text{Cl}_2]$	34.7		-180.7 q	17.2	-594.4
3	$\text{Ph}_3\text{P}(\text{CH}_2)_3\text{Cl}[\text{VO}_2\text{Cl}_2]$	34.7		-180.7 q	16.9	-594.4
4	$\{p\text{-BrC}_6\text{H}_4\text{CH}_2\text{P}[\text{N}(\text{CH}_2\text{CH}_3)_2]_3\}[\text{VO}_2\text{Cl}_2]$	34.4		-181.7 q	16.8	-594.5
5	$\text{Ph}_3\text{P}(\text{CH}_2)_2\text{PPh}_3[\text{VO}_2\text{Cl}_2]_2$	34.4		-181.7 q	17.2	-594.3
6	$\text{Ph}_3\text{P}(\text{CH}_2)_4\text{PPh}_3[\text{VO}_2\text{Cl}_2]_2$	34.7		-181.7 q	16.9	-594.2
7	$\text{Ph}_3\text{P}(\text{CH}_2)_5\text{PPh}_3[\text{VO}_2\text{Cl}_2]_2$	34.7		-180.7 q	16.3	-594.4

reaction mixture between  $\text{KF}$  and phosphonic acid exhibit two signals, one at  $-176$  ppm corresponding to the formation of  $\text{HF}$  and the other to the formation of  $\text{BF}_4^-$  (see above). It should be noted that there is no  $^{19}\text{F}$  NMR signal for both  $\text{KF}$  and  $\text{KF} + \text{M}[\text{VO}_2\text{Cl}_2]$  in a  $\text{CD}_3\text{CN}$  solution because of the low solubility of  $\text{KF}$  in  $\text{CD}_3\text{CN}$ .

**Figure 6.** Multinuclear NMR spectra of the reaction mixture of  $\text{Ph}_3\text{P}(\text{CH}_2)_2\text{PPh}_3[\text{VO}_2\text{Cl}_2]$  (0.1 mmol),  $\text{KF}$  (in excess as a solid), and  $\text{MePO}_3\text{H}_2$  (0.06 mmol) in  $\text{CD}_3\text{CN}$  at room temperature: (a)  $^{19}\text{F}$  NMR; (b)  $^{31}\text{P}$  NMR; (c)  $^{51}\text{V}$  NMR (chemical shifts in ppm).

From the above-mentioned facts, it becomes clear that  $^{31}\text{P}$ ,  $^{19}\text{F}$ , and  $^{51}\text{V}$  NMR spectra indicate the formation and existence of the cage compound in solution. The formation of the cage structure is energetically favored<sup>10</sup> and is fast enough that other vanadium species could not be observed when an excess of phosphonic acid and  $\text{KF}$  were used. Therefore, it must be stated that no information about intermediates and the reaction mechanisms of the cage formation could be obtained from multinuclear NMR spectroscopy under the applied reaction conditions.

To obtain more information about the formation of the cage structure, two other systems have been studied. In the first one, an excess of  $\text{M}[\text{VO}_2\text{Cl}_2]$  was used in comparison with  $\text{MePO}_3\text{H}_2$  and  $\text{KF}$ . As shown in Figure 6, the  $^{31}\text{P}$  and  $^{19}\text{F}$  NMR spectra exhibit only the signals that were attributed to the cage compound, while the  $^{51}\text{V}$  NMR spectrum exhibits two signals, one corresponds to the formation of the cage structure and the other to the vanadium precursor compound. There is no indication about the formation of other species. In a second experiment, an excess of  $\text{MePO}_3\text{H}_2$  and  $\text{KF}$  was used in comparison with that of  $\text{M}[\text{VO}_2\text{Cl}_2]$ . As shown in Figure 7, both  $^{31}\text{P}$  and  $^{19}\text{F}$  NMR spectra exhibit the signals that were assigned to the formation of the cage structure as well as to species produced from the interaction of excess  $\text{MePO}_3\text{H}_2$  and  $\text{KF}$ , while the  $^{51}\text{V}$  NMR spectrum exhibits only one signal attributed to the formation of the cage structure.

Concerning the role of the charge-compensating groups in the formation of the cage structures  $[(\text{V}_2\text{O}_3)_2(\text{RPO}_3)_4\text{CF}]^-$ , different phosphonium ions that have specific charge, shape, size, and functional groups were used, namely,  $\text{Ph}_4\text{P}^+$ ,  $\text{Ph}_3\text{PEt}^+$ ,  $^t\text{Bu}_4\text{P}^+$ ,  $(\text{Et}_2\text{N})_3\text{PCH}_2\text{Ph}^+$ ,  $\text{Ph}_3\text{P}(\text{CH}_2)_3\text{Cl}^+$ ,  $\text{Ph}_3\text{P}(\text{CH}_2)_4\text{Cl}^+$ ,  $\text{Ph}_3\text{PCH}_2\text{OCH}_3^+$ ,  $\text{Ph}_3\text{P}(\text{CH}_2)_2\text{PPh}_3^{2+}$ , and  $\text{Ph}_3\text{P}(\text{CH}_2)_4\text{PPh}_3^{2+}$ .

As shown in Table 3, there is no or a very small change in the positions of  $^{19}\text{F}$ ,  $^{31}\text{P}$ , and  $^{51}\text{V}$  NMR signals for the corresponding cage compounds that have different counter-cation, which means that there is no relevant influence of the size, shape, and charge of the counter-cations on the formation of the tetranuclear vanadium phosphonate cage structures in the presence of a fluoride ion, which was shown in the reaction with methylphosphonic acid. The chemical shifts of  $^{19}\text{F}$ ,  $^{31}\text{P}$ , and  $^{51}\text{V}$  NMR signals are governed by the geometry, electron density distribution, and induced interactions of the cage.

**Redox Activity of the Cage Compounds.** With respect to possible applications, the redox activities of the cages

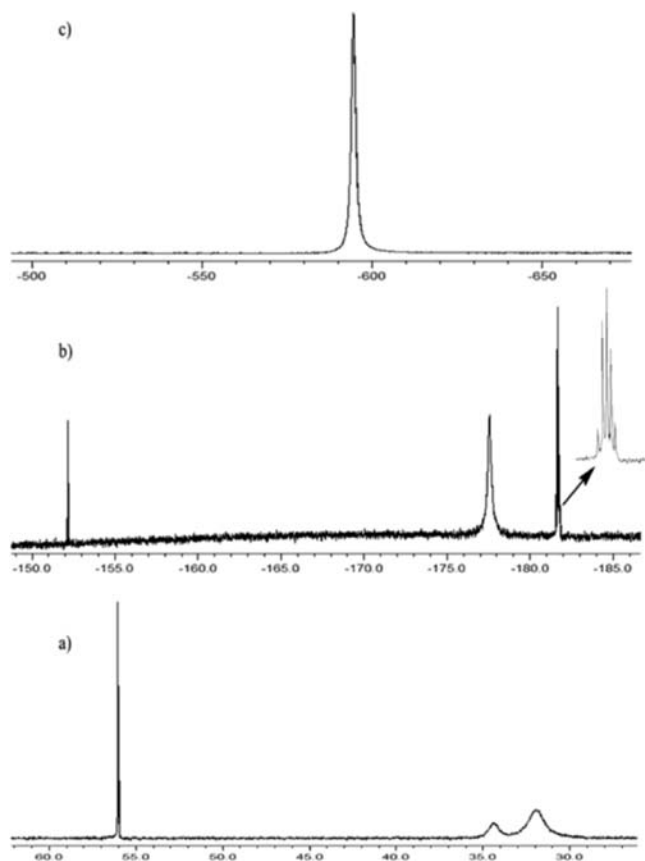


**Figure 7.** Multinuclear NMR spectra of the reaction mixture of  $[(\text{CH}_3\text{CH}_2)_2\text{N}]_3\text{PCH}_2\text{Ph}[\text{VO}_2\text{Cl}_2]$  (0.07 mmol), KF, and  $\text{MePO}_3\text{H}_2$  (0.1 mmol) in  $\text{CD}_3\text{CN}$  at room temperature: (a)  $^{31}\text{P}$  NMR; (b)  $^{19}\text{F}$  NMR; (c)  $^{51}\text{V}$  NMR (chemical shifts in ppm).

$\text{M}^{n+}[(\text{V}_2\text{O}_3)_2(\text{RPO}_3)_4\text{CF}]_n$  were studied on the basis of the EPR spectra taken in solution as well as in the solid state. The cage itself ( $4\text{V}^{\text{V}}$ ) without the fluoride anion would be neutral. However, the encapsulation of the fluoride anion results in the formation of an anionic cage fragment, which is balanced by a counteranion to maintain electroneutrality. Because of the possibility of the preparation of cage compounds with different counteranions, it was of interest to study to what extent the chemical and physical properties (such as the solubility, spectral behavior, and redox properties) could be modified by changing the organic moieties of either the phosphonate or the cationic fragments. Phosphonium ions are suitable charge-compensating groups because of the possibility of incorporating a variety of functional groups into their organic moieties with different chemical properties, which may be imparted to the final product, they are easily introduced into vanadium species, they are easy to prepare with specific size and charge, and they have an important role in the formation of crystalline compounds, which makes recrystallization of the final product easier. Whereas evidence for the existence of the cages in solutions can easily be given by multinuclear NMR for the diamagnetic state ( $4\text{V}^{\text{V}}$ ) and by EPR for the paramagnetic state ( $3\text{V}^{\text{V}}/\text{V}^{\text{IV}}$ ), it is a great challenge to give evidence for the existence of the (undestroyed) cage at redox reactions in the solid state.

To apply EPR to this problem, cages in the doublet state ( $S = 1/2$ ) must be generated in the solid state. After EPR

measurements, the cage should be reoxidized or transferred to solution to guarantee that the structure withstands the procedure. For this purpose, the reduction was performed in two ways: (i) using the thermal energy provided by TGA for driving the internal redox reactions, which can be subsequently monitored by ESR, and (ii) performing the reduction by  $\text{H}_2$  activated on the surface of platinum powder in situ directly in the EPR cavity. The experiments doubtlessly show the reversible reduction/oxidation of the cage compounds at room temperature in the solid state. This means, in contrast to many redox processes performed with solid catalysts containing transition-metal ions, here we can refer to *identified* molecular structures that exist in solution and in the solid state too. Corresponding to the aim of this work, we have with this molecular approach the possibility to study the redox activity of vanadium compounds on a molecular level as well as in solution and in the solid state on a defined redox system.

**Thermally and Chemically Induced Reactions of the  $\text{V}^{\text{V}}$ /Cage Compounds.** Starting from the interesting and, in part, unexpected results obtained by silver-mediated reactions of the cage compounds,<sup>11</sup> the question of the influence of *non-transition-metal* cations on the redox chemistry is raised. Therefore, combined TGA and EPR measurements were performed. In addition, the chemical reactions in solution and in the solid state were watched by EPR. It was the goal of this kind of investigation to find (i) how the cages will be modified (e.g., by formation of  $\text{V}^{\text{IV}}$  ions inside the cages) and (ii) at which temperature they will be transformed in another reactive species or destroyed. The last mentioned aspect is of special interest for a potential application of the compounds.<sup>11</sup>

To study the thermal behavior of these materials, four compounds with different organic substituents either of counteranions or of the phosphonate ligands of the cage structure have been chosen, namely,  $[(\text{Et}_2\text{N})_3\text{PCH}_2\text{Ph}][(\text{V}_2\text{O}_3)_2(\text{PhPO}_3)_4\text{F}]$ ,  $[\text{Ph}_3\text{P}(\text{CH}_2)_2\text{PPh}_3][(\text{V}_2\text{O}_3)_2(\text{PhPO}_3)_4\text{F}]_2$ , and  $\{\text{Ph}_4\text{P}[(\text{V}_2\text{O}_3)_2(\text{PhPO}_3)_4\text{F}] \cdot \text{CH}_3\text{CN}\}$ , which have different phosphonium ions as charge-compensating groups in addition to  $\text{Ph}_4\text{P}[(\text{V}_2\text{O}_3)_2(\text{MePO}_3)_4\text{CF}] \cdot 2\text{CH}_3\text{CN}$ . The TGA/differential thermogravimetry (DTG; Figure 8) curves show that the compound  $\{\text{Ph}_4\text{P}[(\text{V}_2\text{O}_3)_2(\text{PhPO}_3)_4\text{F}] \cdot \text{CH}_3\text{CN}\}$  is stable up to  $\sim 340^\circ\text{C}$ , which indicates that the cage should retain its structure up to this temperature. However, at higher temperatures (in the range of  $345\text{--}375^\circ\text{C}$ ), the first two weight losses may correspond to the removal of  $\text{CH}_3\text{CN}$  and fluoride, which implies a destruction of the cage structure because the fluoride anion should not be released from the intact cage structure. The weight losses (obsd 4.24%; calcd 4.53%) are overlapping together, as seen in the DTG curve, and are associated with endothermic processes. The other weight losses at higher temperatures should be attributed to the pyrolysis of the organic fragments.

Compound  $[\text{Ph}_3\text{P}(\text{CH}_2)_2\text{PPh}_3][(\text{V}_2\text{O}_3)_2(\text{PhPO}_3)_4\text{F}]_2$  displayed thermal stability up to  $\sim 260^\circ\text{C}$ , which indicates that the cage compound retained its structure up to this temperature. However, it is difficult to give a clear answer about the existence of the cage structure beyond this temperature.



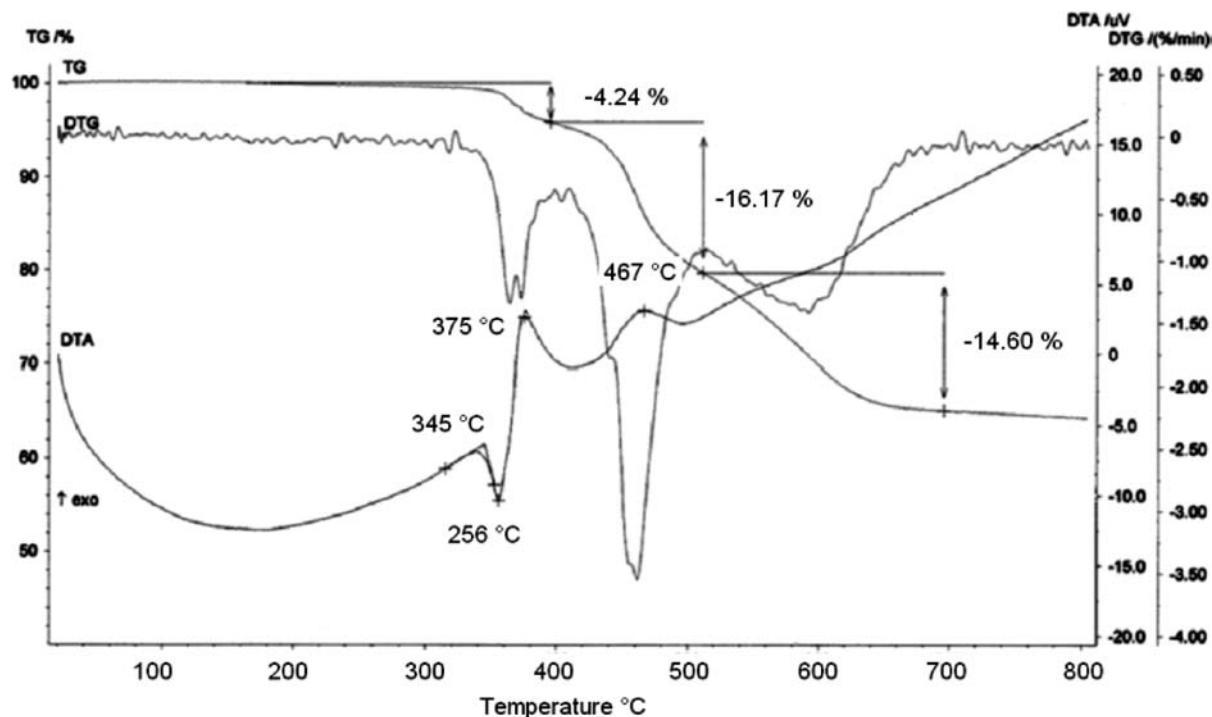


Figure 8. TGA/DTG of  $\{\text{Ph}_4\text{P}[(\text{V}_2\text{O}_3)_2(\text{PhPO}_3)_4\text{F}] \cdot \text{CH}_3\text{CN}\}$ .

The TGA/DTG curves of compound  $[(\text{Et}_2\text{N})_3\text{PCH}_2\text{Ph}][(\text{V}_2\text{O}_3)_2(\text{PhPO}_3)_4\text{F}]$  display thermal stability up to  $\sim 240^\circ\text{C}$ . However, there is a sharp weight loss (4.23%) at about  $275^\circ\text{C}$  associated with exothermic processes, which should be attributed to the action of the amino-substituted phosphonium ion. The other weight losses should again be attributed to pyrolysis of the organic fragments. The different thermal behavior of  $[(\text{Et}_2\text{N})_3\text{PCH}_2\text{Ph}][(\text{V}_2\text{O}_3)_2(\text{PhPO}_3)_4\text{F}]$  must be attributed to the presence of amino groups in the phosphonium ion, which should be responsible for initiating an effective redox reaction, as was evidenced from EPR measurements (see the EPR part). The role of amino groups as a reducing agent was confirmed from separate experiments in which  $\text{NH}_4\text{F}$  was used as a reducing agent. The TGA of  $[\text{Ph}_4\text{P}][(\text{V}_2\text{O}_3)_2(\text{MePO}_3)_4\text{F}] \cdot 2\text{CH}_3\text{CN}$  has been studied and compared with that of  $[\text{Ph}_4\text{P}][(\text{V}_2\text{O}_3)_2(\text{PhPO}_3)_4\text{F}] \cdot \text{CH}_3\text{CN}$  because they have the same counterions but different organic substituents of the cage structures. TGA coupled with mass spectrometry indicates that the first weight loss is attributed to the removal of the part of  $\text{CH}_3\text{CN}$  associated with an endothermic process. As is evident from the corresponding EPR measurement, this weight loss is not associated with a reduction process of the cage structure. However, at temperatures above  $330^\circ\text{C}$ , a second weight loss appears, which was attributed to the release of a second  $\text{CH}_3\text{CN}$  molecule (obsd 3.16%; calcd 3.67%). It seems to be that the cage retained its structure up to this temperature,  $\sim 330^\circ\text{C}$ .

Generally, the thermally induced redox process of the cage compounds in solids can be summarized by three main steps. First, the formation of isolated  $\text{V}^{\text{IV}}$  centers occurs; in these cases, the EPR spectra exhibit eight-line spectra with axial features typical for the solid-state spectrum of the paramagnetic cage.<sup>10</sup> The appearance of the paramagnetism is

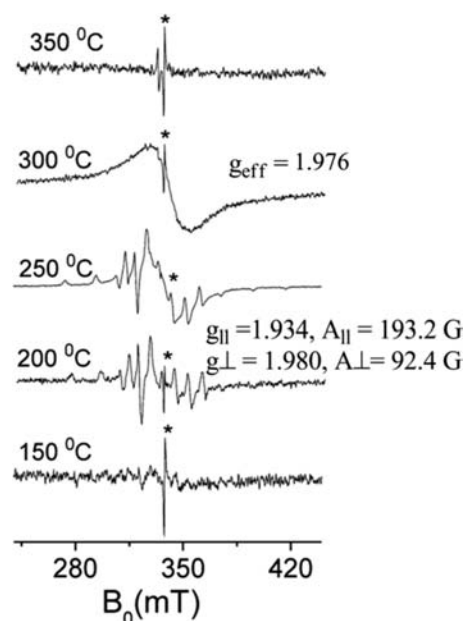


Figure 9. EPR spectra of  $\{[(\text{CH}_3\text{CH}_2)_2\text{N}]_3\text{PCH}_2\text{Ph}\}[(\text{V}_2\text{O}_3)_2(\text{PhPO}_3)_4\text{CF}]$  (0.2 mmol) taken at  $20^\circ\text{C}$  after different thermal treatments. \*Reference:  $\text{MgO}:\text{Cr}^{3+}$ ,  $g = 1.9796$ .

temperature-dependent because of the presence of different phosphonium ions that are involved in the redox reactions. Second, because the amount of  $\text{V}^{\text{IV}}$  centers increases with the temperature, the EPR signals become broad with a gradual loss of their hyperfine splitting (Figure 9).

The lack of a well-resolved hyperfine structure by line-width broadening indicates that the  $\text{V}^{\text{IV}}$  centers exert some degree of magnetic dipolar interactions. Third, when different paramagnetic vanadium centers are close enough to form common spin states (e.g., at  $300\text{--}450^\circ\text{C}$ ), the EPR intensity starts to decline and drops off as the sample is further heated.



The drop-off of the EPR signal may be attributed to the presence of a strong magnetic exchange between the interacting  $V^{IV}$  ions. However, there is another possibility for such behavior in which  $V^{IV}$  is reduced to  $V^{III}$ , which is EPR-silent under these conditions. The temperatures at which the EPR signals appeared and disappeared are chemically dependent on the types of counterions.

**Reduction of the Cage in Solution.** It has been reported that the cage compound  $[(V_2O_3)_2(PhPO_3)_4CF]^-$  shows reversible one-electron reductions at +0.06 and -0.56 V with respect to the ferrocene/ferrocenium.<sup>8</sup> Using  $I^-$  or  $H_2$  activated on the surface of platinum in  $CH_3CN$ , the one-electron transfer to the cage structure  $[(V_2O_3)_2(RPO_3)_4CF]^-$  results in the formation of paramagnetic species. The corresponding EPR spectra of the cage structures in the doublet state are due to a pattern of 29 hyperfine lines because of the interaction of the unpaired electron with four approximately equivalent  $^{51}V$  nuclei ( $I = 7/2$ ). In the case when the spectral resolution depends on the viscosity of the used solvent,<sup>25</sup> a higher temperature ( $\sim 80^\circ C$ ) is necessary for a complete spectral resolution due to a certain extent interactions between the cages and the solvent, which are dependent on the structural orientations of the molecules, like hydrogen bonding. A 29-line spectrum gives evidence for a complete delocalization of the spin density inside the cages.

With a change in the reducing agents, a further interesting effect could be established. Two electron-rich heteroaromatics have been selected for this purpose because they fulfill the following conditions: (i) they perform the one-electron reduction of the cage and (ii) at the same time they contribute to a differentiation of the solvent effects with respect to the tumbling rate of the cages with  $S = 1/2$  and the hopping rate of the unpaired electron and therefore to the delocalization of the spin density inside the cage, and last but not least they can cause additional and specific interactions (e.g., via hydrogen bonding).

**Reduction of the Cage by Quinoline in  $CH_3CN$  and DMSO.** At room temperature, a broad and not well-resolved EPR signal was obtained that enhances its spectral resolution to a 29-line hyperfine structure at  $80^\circ C$  (Figure 10). This means that the broad line represents the envelope of this hyperfine pattern, which is resolved at higher tumbling rate and indicates the complete spin-density delocalization inside the cages.

**Reduction of the Cages by 1-Methylimidazole.** The EPR spectrum (Figure 11) of the cage  $[(V_2O_3)_2(PhPO_3)_4CF]^-$  in a  $CH_3CN$  solution treated with 1-methylimidazole yields an eight-line pattern exhibiting some magnetic anisotropy and broadening of the individual transition. This hyperfine pattern must be attributed to the interaction of the unpaired electron with only one  $^{51}V$  nucleus. This means that, under this condition, an essential localization of the spin density has taken place. When the solution is heated up to  $80^\circ C$ , the spectral resolution will be improved and a broad EPR transition appears, indicating the progressive delocalization

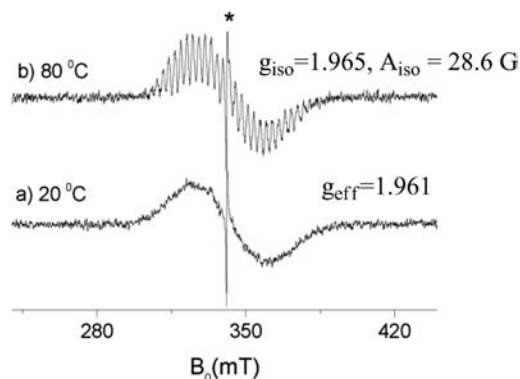


**Figure 10.** EPR spectra of  $Ph_4P[(V_2O_3)_2(PhPO_3)_4CF] \cdot CH_3CN$  (0.05 mmol) after reduction with quinoline (2 mmol) in DMSO taken at different temperatures. \*Reference:  $MgO:Cr^{3+}$ ,  $g = 1.9796$ .

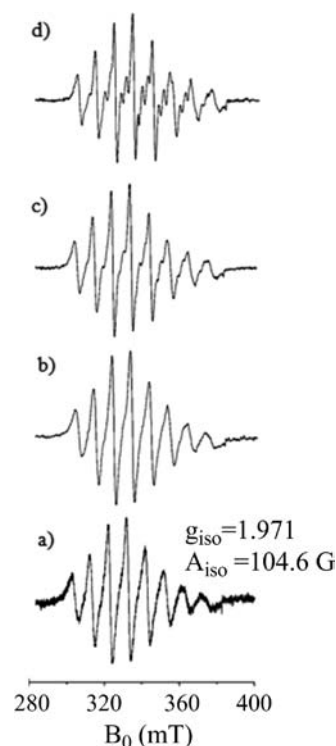


**Figure 11.** EPR spectra of  $[(V_2O_3)_2(PhPO_3)_4CF]^-$  (0.05 mmol) after reduction with 1-methylimidazole (2 mmol) in  $CH_3CN$  taken at different temperatures: (a)  $20^\circ C$ ; (b)  $40^\circ C$ ; (c)  $60^\circ C$ ; (d)  $80^\circ C$ .

of the spin density inside the cages (see, e.g., the line splitting in Figure 11c,d). 1-Methylimidazole is rather able to form a specific interaction with the reduced cages,<sup>10</sup> which not only diminishes the tumbling rate of the cage in the doublet state but also forces nonaveraged specific interactions based on hydrogen bonds. As a consequence, the localization of the spin density is essentially at one  $^{51}V$  nucleus of the cage.

The studies performed on thermally induced changes of the cage compounds in the solid state lead to the formation of  $V^{IV}$  species that exhibit a single Lorentzian line at the  $g = 1.976$  due to the effective spin exchange between the associated species. However, it could not be decided whether the origin of this spin exchange results from the interaction of two (or more) different interacting but intact cages or from the exchange interactions of the  $V^{IV}$  ions of thermally destroyed cages.

(25) Guzy, M.; Raynor, J. B.; Symons, M. C. R. *J. Chem. Soc. A* **1969**, 279, 1–2795.

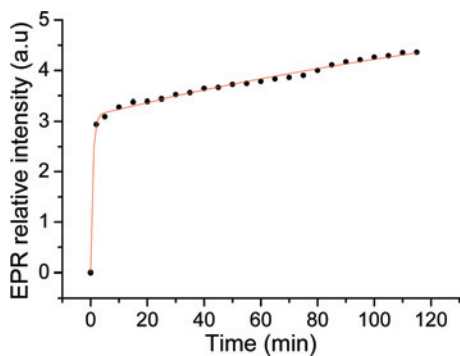


**Figure 12.** EPR signal intensities vs time for the reduction of  $\text{Ph}_4\text{P}[(\text{V}_2\text{O}_3)_2(\text{PhPO}_3)_4\text{CF}]$  (0.2 mmol)/platinum powder (0.05 g) under a flow of  $\text{H}_2$  at room temperature and ambient pressure.

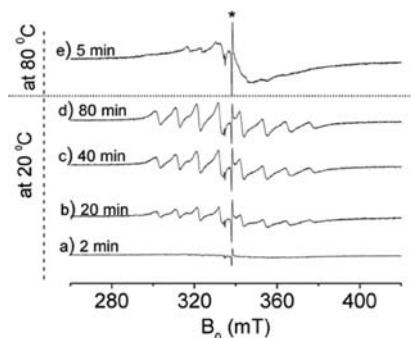


**Figure 13.** The EPR spectra for the reduction of  $\text{Ph}_4\text{P}[(\text{V}_2\text{O}_3)_2(\text{PhPO}_3)_4\text{CF}]$  (0.2 mmol) /Pt-powder (0.05 g) under flow of  $\text{H}_2$  as function of time and temperature at ambient pressure.

**Reduction of the Cage Compounds in the Solid State.** Attempts to reduce the cage of the title compounds in the solid state lead to questions (i) for the existence of the intact cages in the doublet states under these conditions and (ii) for the extent of magnetic coupling between intact doublet cages in the solid state. Even the last problem mentioned cannot easily be separated from interactions of released  $\text{V}^{\text{IV}}$  ions upon destruction of the cages in the run of thermal reduction at higher temperature. Therefore, the reduction of the cages was performed at 20 °C using a mixture of the solid cage compound with platinum powder. This mixture was flushed with  $\text{H}_2$  directly in the cavity of the EPR spectrometer. The results are shown in Figures 12 and 13.

This offers four remarkable findings: (i) the reduction really proceeds under these conditions at room temperature,

(ii) an eight-line spectrum results because of the deformation of the cages by packing effects in the solid state, (iii) the yield of the reduction reaction depends on the substituents R of the cage, and finally (iv) at a certain time interval, where the concentration of paramagnetic cages ( $3\text{V}^{\text{V}}/\text{V}^{\text{IV}}$ ) is high enough, spin exchange will be effective and an eight-line spectrum tends to collapse into a single-line spectrum by cage–cage interaction. This means that the cage remains intact at the transformation into the doublet ( $S = 1/2$ ) state even in the solid state. This statement is strongly supported by the fact that dissolution of the  $\text{H}_2$ -treated solid in  $\text{CH}_3\text{CN}$  yielded the expected 29-line spectrum of the freely tumbling doublet cages.

## Conclusions

The present paper reports on a new and very simple preparative method for the preparation of tetranuclear cage compounds with the general formula  $\text{M}^{n+}[(\text{V}_2\text{O}_3)_2(\text{RPO}_3)_4\text{CF}]_n$ . This method allows the preparation of these compounds in a great variety with high yields and therefore provides the possibility of tuning the properties like solubility or thermal stability.

Thus, for the first time, it was possible to study the redox behavior of these compounds on a molecular level as well as in solution and in the solid state.

Especially, the investigation of the redox reaction of defined molecular clusters with  $\text{H}_2$  in the solid state as (molecular approach) has been carried out in a unique way to study such kinds of reactions, which are important for the basic understanding of catalytic processes.

**Acknowledgment.** The DAAD is acknowledged for financial support to J. K. Jabor, A. Thies, W.-D. Bloedorn, H. Vogt, and M. Päch are acknowledged for supporting this work.

**Supporting Information Available:** Crystallographic data in CIF format for  $\text{Ph}_4\text{P}[(\text{V}_2\text{O}_3)_2(\text{MePO}_3)_4\text{CF}] \cdot 2\text{CH}_3\text{CN}$ ,  $\text{Ph}_4\text{P}[(\text{V}_2\text{O}_3)_2(\text{PrPO}_3)_4\text{CF}]$ , and  $\text{Ph}_4\text{P}[(\text{V}_2\text{O}_3)_2(\text{PhPO}_3)_4\text{CF}] \cdot \text{CH}_3\text{CN}$  as well as thermal analyses and EPR measurements for  $\text{Ph}_4\text{P}[(\text{V}_2\text{O}_3)_2(\text{MePO}_3)_4\text{CF}] \cdot 2\text{CH}_3\text{CN}$ ,  $\text{Ph}_4\text{P}[(\text{V}_2\text{O}_3)_2(\text{MePO}_3)_4\text{CF}] \cdot 2\text{CH}_3\text{CN}$ ,  $\text{Ph}_3\text{P}(\text{CH}_2)_2\text{PPh}_3[(\text{V}_2\text{O}_3)_2(\text{PhPO}_3)_4\text{F}]_2$ , and  $[(\text{Et}_2\text{N})_3\text{PCH}_2\text{Ph}]_3[(\text{V}_2\text{O}_3)_2(\text{PhPO}_3)_4\text{F}]$ . This material is available free of charge via the Internet at <http://pubs.acs.org>.

IC800707V